ИНСТИТУТ ЯДЕРНОЙ ФИЗИКИ СО АН СССР

V.P.Druzhinin, M.S.Dubrovin, S.I.Eidelman,
V.B.Golubev, V.N.Ivanchenko, R.M.Ivanov,
G.Ya.Kezerashvili, I.A.Koop, A.P.Lysenko,
E.V.Pakhtusova, E.A.Perevedentsev, A.N.Peryshkin,
A.A.Polunin, I.Yu.Redko, S.I.Serednyakov,
Yu.M.Shatunov, V.A.Sidorov, A.N.Skrinsky,
Yu.V.Usov, I.B.Vasserman, P.V.Vorobyov

RECENT RESULTS OF EXPERIMENTS WITH THE NEUTRAL DETECTOR AT VEPP-2M

PREPRINT 84-93

НОВОСИБИРСК

Abstract

Preliminary results of experiments with the Neutral Detector at the VEPP-2M electron-positron collider are presented for the c.m. energy range 1000÷1400 MeV. The following Φ-meson branching ratios have been measured (the former for the first time):

$$B(\Phi\to\eta e^+e^-)=(1.3^{+0.5}_{-0.6})\cdot 10^{-4}$$

$$B(\Phi\to\pi^+\pi^-)=(0.7^{+0.4}_{-0.3})\cdot 10^{-4}$$

Processes with 1, 3, 4 and 5 final photons have been investigated. The following upper limits have been placed at 90% confidence level:

$$B(\Phi\to\pi^0\pi^0\gamma)<8\cdot 10^{-3}$$
$$B(\Phi\to\pi^0\eta\gamma)<5\cdot 10^{-3}$$
$$\sigma(e^+e^-\to\pi^0\pi^0)<0.2\ \text{nb}$$
$$\sigma(e^+e^-\to\pi^0\eta)<0.1\ \text{nb}$$
$$\sigma(e^+e^-\to X\gamma)<0.3\ \text{nb}$$

where X is a hypothetical boson with a mass not greater than 200 MeV not observed in the Neutral Detector.
The reaction $e^+e^-\to\omega\pi^0\to\pi^0\pi^0\gamma$ has been studied and compared with the previously measured reaction $e^+e^-\to\pi^+\pi^-\pi^0\pi^0$.

This work presents preliminary results of two experiments performed at the electron-positron collider VEPP-2M [1] with the Neutral Detector [2]. The first experiment was performed in the centre-of-mass energy range $2E_0$ from 1000 up to 1050 MeV, i.e. near the Φ-meson. Some results of this experiment have already been published in Refs. [3-5]. The second one covered the range $2E_0$ from 1050 up to 1400 MeV.

DETECTOR AND EXPERIMENT

The scheme of the detector is shown in Fig.1. Its main part is an electromagnetic calorimeter consisting of 168 scintillation counters with NaI(Tl) crystals (total weight about 2.6 tons). The minimum thickness is 12 radiation lengths. The central tracking system for charged particles consists of three layers of two-coordinate cylindrical proportional chambers. Between NaI(Tl) crystals two layers of two-coordinate proportional chambers are installed to measure photon angles (shower chambers). Outside the calorimeter there is an iron absorber 10 cm thick and anticoincidence scintillation counters to suppress a cosmic background. A total solid angle of the detector is 65% of 4π. The detector calibration is performed using cosmic muons. The energy resolution for electrons and photons is determined by the amount of passive material between NaI(Tl) crystals and in the energy range of 50—1000 MeV the resolution is 25-10% (FWHM). The angular resolution for photons is 1.5° (RMS) in the azimuthal direction and 3.5° (RMS) for the polar angle. For charged particles it is 0.5° and 2° respectively. For exclusive channels the detector resolution can be improved [2] using the kinematic fit [6].

In both experiments the cited energy range was scanned. For the first one a scanning step was 0.5 MeV, the integrated luminosity was 3 pb^{-1}, the total number of recorded events was about $1.3\cdot 10^7$, $0.3\cdot 10^7$

of which being due to Φ-meson decays. The absolute calibration of the energy scale was performed using an excitation curve in the channel $\Phi\to K_L K_S\to$neutrals and table value of the Φ-meson mass [7]. To this end events having four or more photons have been selected. The luminosity was determined with a 2% accuracy using events of Bhabha scattering and two-photon annihilation at large angles.

In the second experiment a step in the average energy was 4 MeV. Within this interval of the beam energy was scanned to and fro with a frequency 0.02 Hz and an amplitude 2.2 MeV. The integrated luminosity was 3.2 pb^{-1}, the number of recorded events about 10^7. The luminosity as in the first experiment was determined by two methods. Fig.2 shows the energy dependence of the ratio of luminosities obtained by two cited methods. To reduce the time of subsequent analysis only each fourth event of Bhabha scattering was recorded in this experiment. Here we present results of the analysis based on approximately one half of the data sample collected in the energy range between 1050 and 1400 MeV.

DECAY MODE $\Phi\to\pi^+\pi^-$

This decay mode was first observed at VEPP-2M by the OLYA detector [8]. The Neutral Detector preliminary results on this mode are described below. The decay reveals itself as an interference in the energy dependence of the cross section of the reaction $e^+e^-\to\pi^+\pi^-$ near the Φ-meson.

At the first stage of analysis events with two collinear tracks in proportional chambers have been selected:

$$|\Delta\varphi|<3^\circ, \qquad |\Delta\theta|<15^\circ \tag{1}$$

where $\Delta\varphi$, $\Delta\theta$ are the acollinearity angles in the azimuthal and polar directions respectively. The following processes can produce a background:

$$e^+e^-\to e^+e^- \tag{2}$$
$$e^+e^-\to\mu^+\mu^- \tag{3}$$
$$e^+e^-\to\Phi\to K_S K_L, K_S\to\pi^+\pi^- \tag{4}$$
$$e^+e^-\to\Phi\to\pi^+\pi^-\pi^0 \tag{5}$$

Charged kaons from the mode $\Phi\to K^+K^-$ do not punch through the tracking system, not giving thereby two collinear tracks.

At the second stage of analysis pion events have been selected:

1) To suppress the background due to the reaction (2) a e/π separation method was used based on the difference in the energy deposited in NaI(Tl) layers for electrons and pions [9].
2) The greater part of muons due to the reaction (3) fires anticoincidence counters and does not produce a trigger. To suppress this process additionally the events in which both particles have an energy deposition in all four NaI(Tl) layers were rejected.
3) The criteria (1) select events of the reaction (4) with two pions having the energy much less than that in the process under study. K_L-meson moving in the direction of one of the pions can produce a large pulse height in the calorimeter. To suppress such background only those events were selected in which one ot the particles met the following conditions:
   - all four layers of NaI(Tl) were fired with a 10 MeV threshold,
   - the energy deposition in the first layer is less than 40 MeV,
   - the energy deposition in the second layer is less than 50 MeV.

The detection cross sections for the processes (2—5) before and after above cuts are given in Table 1.

The remaining background did not exceed 7% of the detection cross section for the process under study and was statistically subtracted. To this end the calculated cross section of the process (3) taking into account the interference with the decay $\Phi\to\mu^+\mu^-$ has been used. As processes (4) and (5) do not give a peak at $\Delta\varphi=0$ their contribution was determined using quasicollinear events with

$$3^\circ<|\Delta\varphi|<6^\circ, \qquad |\Delta\theta|<15^\circ$$

The coefficient allowing the recalculation from quasicollinear to collinear events (1) was determined by Monte Carlo.

About 20000 events have been selected under these criteria, the number of background events in this sample being about 900. The following formula was used to parametrize the energy dependence of the experimental cross section [8]:

$$\sigma(E)=\frac{\pi\alpha^2}{12E^2}\left(\frac{\beta}{\beta_\Phi}\right)^3|F_\pi|^2(1+A(E-m_\Phi/2))\times$$

$$\times\left|1+\frac{Q\,e^{i\psi}\,m_\Phi\Gamma_\Phi}{4E^2-m_\Phi^2+im_\Phi\Gamma_\Phi}\right|^2\cdot\varepsilon(1-\delta)+\sigma_b(E)$$

$$\beta=(1-m_\pi^2/E^2)^{1/2}, \qquad \beta_\Phi=(1-4m_\pi^2/m_\Phi^2)^{1/2},$$

where Q and ψ are the amplitude and phase of interference, F_π, A are the pion formfactor and its slope in the resonance maximum, ε is the detection efficiency, δ is the radiative correction [10,11], $\sigma_b(E)$ is the detection cross section for background processes. The interference amplitude Q is connected with the branching ratio as follows:

$$Q=\sqrt{\frac{36B(\Phi\to e^+e^-)\cdot B(\Phi\to\pi^+\pi^-)}{\alpha^2\beta_\Phi^3|F_\pi|^2}}$$

parameters $|F_\pi|^2$, A, ψ, Q were determined by the fit. Experimental values of the detection cross section and the optimum curve are shown in Fig.3. χ^2 for the curve is 18 at 20 degrees of freedom, whereas the fit with $Q=0$ gives χ^2 equal to 39 at 22 degrees of freedom ($P(\chi^2)<0.02$). The following values of parameters have been obtained from the fit:

$$|F_\pi|^2=2.1\pm0.2$$
$$Q=0.08\pm0.02$$
$$B(\Phi\to\pi^+\pi^-)=(0.6\pm0.3)\cdot10^{-4}$$
$$\psi=(-41\pm12)^\circ$$

The above value of the formfactor is by two standard deviations lower than in Refs. [8,12]. This difference can probably be due to a systematic uncertainty in the detection efficiency associated with the simulation of the nuclear interaction of pions in the detector. Q and ψ do not depend on the detection efficiency and their errors are statistical. If one uses the formfactor value from Ref. [12] $|F_\pi|^2=(2.7\pm0.2)$, the following value of the branching ratio is obtained:

$$B(\Phi\to\pi^+\pi^-)=(0.7^{+0.4}_{-0.3})\cdot10^{-4}$$

Using the same value of $|F_\pi|^2$ and the value of Q from Ref. [8] one obtains:

$$B(\Phi\to\pi^+\pi^-)=(1.7^{+0.9}_{-0.7})\cdot10^{-4}$$

OBSERVATION OF THE DECAY MODE $\Phi\to\eta e^+e^-$

The decay mode $\Phi\to\eta e^+e^-$ is interesting since it allows a study of the transition $\Phi\to\eta\gamma^*$, where γ^* is a virtual photon with a mass $q^2>4m^2$. The decay probability is connected with the probability of the decay $\Phi\to\eta\gamma$ via the following relation [13]:

$$\frac{d}{dm_{ee}^2}\left(\frac{B(\Phi\to\eta e^+e^-)}{B(\Phi\to\eta\gamma)}\right)=\frac{\alpha}{3\pi}\frac{|F(m_{ee}^2)|^2}{m_{ee}^2}\left(1+\frac{2m^2}{m_{ee}^2}\right)\left(1-\frac{4m^2}{m_{ee}^2}\right)^{1/2}\times$$
$$\times\left[\left(1-\frac{m_{ee}^2}{m_\Phi^2-m_\eta^2}\right)^2-\frac{4m_\eta^2m_{ee}^2}{(m_\Phi^2-m_\eta^2)^2}\right]^{3/2}$$

where m_{ee} is the invariant mass of the e^+e^- pair, $F(m_{ee}^2)$ is a transition form factor. The main contribution to the decay probability comes from the region of m_{ee} close to a threshold $m_{ee}=2m$, where the form factor should be unity. Integrating (6) under this assumption one obtains the following estimate for the branching ratio: $B(\Phi\to\eta e^+e^-)=0.8\%$ or $B(\Phi\to\eta e^+e^-)=1.2\cdot10^{-4}$.

The distribution in the angle between electron and positron has a narrow peak at angles close to zero with a peak width about $1/\gamma$, where γ is a Lorentz factor. For 50% of events this angle does not exceed 10°.

For further analysis the following cuts were applied:
- total energy deposition is greater than 700 MeV;
- there are two showers in a calorimeter caused by photons and one caused by one or several charged particles close to each other;
- showers are well separated: the azimuthal angle between each pair is greater than 20°;
- the invariant mass of photons exceeds 300 MeV.

Events satisfying these criteria have been visually scanned at the display. 13 events have been found with two close tracks coming from the interaction region and the azimuthal angle between them being from 3 to 20 degrees. The lower boundary corresponds to the minimum angle at which tracks in coordinate chambers can still be distinguished, and it is determined by the step between the wires. The same final state can appear in the decay $\Phi\to\eta\gamma$, $\eta\to e^+e^-\gamma$ as well as in the QED process of double bremsstrahlung (DB) at large angles. A characteristic feature of the process under study is a fixed mass of a photon pair equal to the η-meson mass. The decay $\Phi\to\eta\gamma$, $\eta\to e^+e^-\gamma$ is characteristic of a monochromatic photon with the energy approximately equal to 360 MeV. For analysis of these processes a scatterplot of Fig.4 can be useful. Its horizontal axis shows the diphoton mass, while a vertical one—the photon energy closest to that of the recoil photon in the decay $\Phi\to\eta\gamma$. The DB process is non-resonant and does not possess peaks in the distributions.

Shown in Fig.4 are experimental (a) and Monte Carlo (b, c) events for the processes $\Phi\to\eta\gamma$, $\eta\to e^+e^-\gamma$ (b) and $\Phi\to\eta e^+e^-$, $\eta\to\gamma\gamma$ (c). Monte Carlo simulation of the processes (b) and (c) was performed using a standard theory of Dalitz decays of vector and pseudoscalar mesons [13]. Bands in the plots mark the regions with more than 90% of Monte Carlo events. Fig.4d shows the expected distribution for the db process. Since the exact formulae for DB with all final particles at large angles are unavailable, the following approximation has been

used. It has been assumed that in the kinematical region where the angle between charged particles is small, the main contribution comes from the diagrams of a three-photon annihilation type with one photon converting in a e^+e^- pair similar to a Dalitz one. The probability of such process calculated per photon was assumed to be equal to the corresponding probability in the η-meson Dalitz decay independently of the photon energy. In this approximation the DB detection cross section is 2 pb and one must observe 5 events of the DB process. However, all 13 experimental events have been found near the Φ-meson maximum, where the expected number of DB events is 2 and less than one event should appear in the region of $\Phi\to\eta e^+e^-$ and $\Phi\to\eta\gamma$. Absence of DB events outside the Φ-meson can be due to the overestimation of the DB detection cross section obtained neglecting scattering diagrams.

One can see that of 13 events presented in Fig.4a 12 can be ascribed to $\Phi\to\eta e^+e^-$ and $\Phi\to\eta\gamma$. Comparison with the Monte Carlo (Fig.4b) shows that the background from $\Phi\to\eta\gamma$ in the region of $\Phi\to\eta e^+e^-$ is about 2. Thus, 7 events of the decay $\Phi\to\eta\gamma$, $\eta\to e^+e^-\gamma$ and 5 of $\Phi\to\eta e^+e^-$, $\eta\to\gamma\gamma$ are observed. Using the Monte Carlo detection efficiencies for these processes the following values for the branching ratios can be obtained:

$$B(\Phi\to\eta e^+e^-)=\frac{n(\Phi\to\eta e^+e^-,\ \eta\to\gamma\gamma)}{N_\Phi\,\varepsilon B(\eta\to\gamma\gamma)}=(1.3^{+0.8}_{-0.6})\cdot 10^{-4}$$

$$B(\Phi\to\eta\gamma)=\frac{n(\Phi\to\eta\gamma,\ \eta\to e^+e^-\gamma)}{N_\Phi\,\varepsilon B(\eta\to e^+e^-\gamma)}=(1.4^{+0.7}_{-0.5})\ \%$$

where $N_\Phi=3.2\cdot 10^6$ is the total number of the Φ decays in the experiment, $\varepsilon=3.2\%$ is the detection efficiency (approximately equal for both processes). Note that $B(\Phi\to\eta e^+e^-)$ differs from 0 at the 97% confidence level.

The obtained value of the branching ratio for the decay mode $\Phi\to\eta e^+e^-$ is in good agreement with the theoretical expectation (6), while the simultaneously measured branching ratio $\Phi\to\eta\gamma$ is in consistence with [4]. To investigate the m_{ee} dependence of the transition form factor a substantial increase of the statistics is needed.

REACTION $e^+e^-\to\gamma\gamma\gamma$

In the c.m. energy range from 1050 to 1400 MeV events with three final photons have been studied. They can be caused by the following reactions:

$e^+e^-\to\gamma\gamma\gamma$ (QED) (7)
$e^+e^-\to\eta\gamma\to\gamma\gamma\gamma$ (8)
$e^+e^-\to\pi^0\gamma\to\gamma\gamma\gamma$ (9)

The background for these processes can come from events of the two-photon annihilation in which one of the photons simulates two due to the shower fluctuations as well as from the processes with a large number of photons like, for example, $e^+e^-\to\omega\pi^0\to\pi^0\pi^0\gamma$ The following cuts have been applied:

- each photon produces a spark in a shower chamber,
- the minimum angle between photons is greater than 30°,
- energy and momentum are conserved.

465 events thus selected correspond to the cross section integrated over the detector solid angle shown in Fig.5a. It is well described by the qed process (7). The background contribution due to the process $e^+e^-\to\omega\pi^0$ is 5%.

In the spectrum of diphoton masses one observes in the energy range between 1050 and 1100 MeV a peak corresponding to the η-meson (Fig.6). Selecting events from this peak one can obtain the total cross section of the reaction (8) (Fig.5b). Its energy dependence does not contradict to the assumption that ϱand Φ-mesons only contribute. The accuracy achieved does not allow determination of the phase of the ϱ-Φ interference.

The process (9) has not yet been selected due to the large background of the two-photon annihilation.

ANALYSIS OF THE PROCESS $e^+e^-\to 4\gamma$

Four photons in the final state can arise due to the following reactions:

$e^+e^-\to\pi^0\pi^0,\ \pi^0\eta\to 4\gamma$ (10)
$e^+e^-\to V\gamma\to P\gamma\gamma\to 4\gamma,\ (V=\varrho,\ \omega,\ \Phi);\ P=\pi^0,\eta)$ (11)
$e^+e^-\to 4\gamma$ (QED) (12)

Reactions (10) are of special interest since they proceed due to the polarizability of neutral π^0 and η mesons [14] and are described by the two-photon exchange diagram of Fig.7. The cross section of the reaction $e^+e^-\to\pi^0\pi^0$ according to Ref. [15] is about 50 pb in the energy range between 600 and 1000 MeV.

In the energy range under study there are two resonances $f(1270)$ and $A_2(1320)$. In colliding beam experiments their branching ratios in two photon decays have been measured to be about 10^{-5}. Hence, one

can estimate their relative electron widths [16]: $B_{ee}=B_{\gamma\gamma}\cdot 10^{-5}=10^{-10}$. Then the expected cross section in a resonance maximum is

$$\sigma(e^{+-}\to f\to\pi^0\pi^0)=0.4 \text{ pb}$$
$$\sigma(e^{+-}\to A_2\to\pi^0\eta)=0.2 \text{ pb}$$

Thus, the contribution of f and A_2-mesons to the reaction (10) is small compared to a non-resonance one.

Reactions of the type (11) represent a so-called «return to the resonance» with the production of a vector meson and a recoil photon at large angles [17]. The main contribution to the cross section of (11) comes from the processes $e^+e^-\to\omega\gamma\to\pi^0\gamma\gamma$ and $e^+e^-\to\Phi\gamma\to\eta\gamma\gamma$. For the angles between 45 and 135 degrees the cross section value is 50 pb at $2E_0=1000\div1100$ MeV and about 15 pb at $2E=1400$ MeV.

Besides reactions (10), (11) and (12) there are processes with a higher multiplicity contributing to a sample of four-photon events:

$$e^+e^-\to\eta\gamma\to\text{neutrals} \quad (13)$$
$$e^+e^-\to K_SK_L\to\text{neutrals} \quad (14)$$
$$e^+e^-\to\omega\pi^0\to\text{neutrals} \quad (15)$$

In these processes many photons are produced, but some of them miss the detector solid angle or merge. Therefore in some cases an event can be recognized as a four-photon one. The following selection criteria have been used:

- each photon fires a spark chamber,
- energy and momentum are conserved.

Under above selection criteria 154 events have been found in the energy range $2E_0$ between 1000 and 1050 MeV. The energy dependence of the corresponding detection cross section shows a clear Φ-meson peak (Fig.8) whose height is accounted for by the contributions of reactions (13) and (14). The non-resonance cross section is about 20 pb and exceeds a sum of expected contributions from reactions (11) and (12) estimated to be 4 pb.

The majority of events with four photons outside the Φ-meson resonance as well as those from the non-resonance background near Φ are determined by the process (15). Spectra of invariant masses of intermediate states as well as the values of cross sections (Fig.9) are in good consistence with this assumption.

Selection of the events due to the reaction (10) was performed for two experiments separately. In the first data sample 33 events outside the Φ-meson have been selected. Further analysis used a scatterplot shown in Fig.10a. Its vertical axis corresponds to a diphoton mass closest to the π^0 mass. This quantity was constructed from 6 possible combinations of photon pairs. A recoil mass is plotted along the horizontal axis. Squares in Fig.10 show the regions of events due to the reaction (10). Under the assumption that this reaction proceeds via a D-wave the detection efficiency for these regions is 2%.

Taking into account the distribution of experimental points (Fig.10a) one can determine the contribution of the background processes in the decribed regions. Using the above value of the detection efficiency one obtains the following upper limits at 90% confidence level:

$$\sigma(e^+e^-\to\pi^0\pi^0)<0.2 \text{ nb}$$
$$\sigma(e^+e^-\to\pi^0\eta)<0.5 \text{ nb}$$

Similarly, the upper limits have been obtained in the energy range between 1050 and 1400 MeV:

$$\sigma(e^+e^-\to\pi^0\pi^0)<0.2 \text{ nb}$$
$$\sigma(e^+e^-\to\pi^0\eta)<0.1 \text{ nb}$$

The obtained values of the upper limits for the reaction $e^+e^-\to\pi^0\pi^0$ are close to theoretical predictions. No calculations exist in literature for the process $e^+e^-\to\pi^0\eta$.

SEARCH FOR DECAY MODES $\Phi\to\pi^0\pi^0\gamma$ AND $\Phi\to\pi^0\eta\gamma$

During the analysis of the Φ-meson data sample events with five final photons have been considered. They can be caused by the following reactions:

$$e^+e^-\to\pi^0\pi^0\gamma$$
$$e^+e^-\to\pi^0\eta\gamma \quad (16)$$

If one assumes that these reactions proceed via $\varrho\pi$ intermediate state only, then using values of $B(\Phi\to\pi^+\pi^-\pi^0)$, $B(\varrho\to\pi\gamma)$ and $B(\varrho\to\eta\gamma)$ [7] one can obtain that the branching ratio of the Φ-decays (16) is not lower than $3\cdot10^{-5}$. According to [18,19] the second reaction in (16) can proceed via $\delta\gamma$ as well.

Reactions (13) and (14) with a large number of final photons can produce the background to (16) since photons can merge or escape detection, giving thereby five detected photons.

For preliminary selection of five-photon events the following criteria were applied:

- at least 4 photons of 5 are accompanied by sparks in shower chambers,

- a photon with the highest energy deposits energy in 3 or 4 NaI(Tl) layers,
- energy and momentum are conserved.

The spectrum of the most energetic photons in selected 454 events is shown in Fig.11. The peak corresponds to the energy of the recoil photon in the reaction (13). Selecting events in the peak one obtains the branching ratio $B(\Phi\to\eta\gamma)=(1.6\pm0.3)\%$ in agreement with our recent results [4].

In the further analysis we have applied the kinematic fit to select events with two final pseudoscalar mesons in a sample of events outside the above peak. To this end all possible combinations of photon pairs have been considered. The detection cross section of the selected events was approximated using the Φ-meson Breit-Wigner curve corrected for radiative effects. The cross section value in a maximum is consistent with the expected contributon of the reaction (13). Therefore one can place upper limits for the branching ratios of decays (16). At 90% C.L. they are:

$B(\Phi\to\pi^0\pi^0\gamma)<8\cdot10^{-3}$
$B(\Phi\to\pi^0\eta\gamma)<5\cdot10^{-3}$

INVESTIGATION OF THE REACTION $e^+e^-\to\omega\pi^0$

The reaction $e^+e^-\to\omega\pi^0$ below 1400 MeV was studied earlier by detectors OLYA [20] and M2N [21] in the main channel of the ω-meson decay $\omega\to\pi^+\pi^-\pi^0$. In our work this reaction is studied using the ω-meson decay via the $\pi^0\gamma$ mode:

$$e^+e^-\to\omega\pi^0\to\pi^0\pi^0\gamma \qquad (17)$$

Although the width of the $\omega\to\pi^0\gamma$ decay is by one order of magnitude smaller, this mode provides the unique identificaton of the $\omega\pi^0$ intermediate state, since other mechanisms do not contribute to the $\pi^0\pi^0\gamma$ final state. On the contrary, for the $\pi^+\pi^-\pi^0\pi^0$ final state $A_1\pi$ and $\rho\pi\pi$ mechanisms contribute as well, resulting in the difficult problem of separating three mechanisms [20].

The reaction (17) was observed in our experiments in events with four and five detected photons. The number of selected four-photon events is listed in Table 2, the corresponding detection cross section—in Fig.9. The selection procedure has already been described above.

The preliminary selection of five-photon events used the criteria of the previous section. Shown in Fig.12 are diphoton masses for 49 events thus selected. A prominent peak at the π^0 mass implies that the majority of events has more than one π^0. This allows selection of 38 events with two π^0 after using all possible combinations of photon pairs.

The spectrum of invariant masses of a photon and π^0 in $\pi^0\pi^0\gamma$ events is shown in Fig.13. Practically all the events can be identified as those of the reaction (17). The number of events in each energy interval is presented in Table 2.

Similarly to the analysis of the four-photon events in the region of the Φ the detection cross section for selected five-photon events was approximated with a Breit-Wigner excitation curve and the non-resonant cross section, the latter being determined by the reaction (17). The value of the cross section in the resonance maximum is accounted for by the contribution of the reaction (13).

The total cross section of the process (17) was obtained combining statistics of four- and five-photon events (Fig.14). The curve shown in the figure represents the theoretical prediction [22] within the vector dominance model with a ρ(770) only.

The obtained results are in good agreement with those of Ref. [20] (Table 2). This allows to draw a conclusion that at the energy below 1400 MeV the $\omega\pi^0$ intermediate mechanism of $\pi^+\pi^-\pi^0\pi^0$ production dominates. The future increase of statistics will allow a detailed study of the energy dependence of the cross section and make conclusions about the existence of ρ′(1250).

SEARCH FOR THE PROCESS $e^+e^-\to X\gamma$

This work continues a search for exotic states X in the reaction $e^+e^-\to X\gamma$ that began in [3]. X can be an axion [23], a supersymmetric boson [24] or a mirror particle [25]. It is assumed that neither X nor the products of its decay are detected. The energy range studied is $2E_0$ between 1050 and 1400 MeV. For analysis events have been selected with one photon coming from the interaction region and firing two layers of shower chambers and three layers of NaI(T!) with a 5 MeV threshold.

473 events with one photon were found in the experiment. Their energy spectrum is presented in Fig.15. As it was shown in ref. [3], the main origins of such photons are the process of large-angle bremsstrahlung at the residual gas in the collider vacuum chamber, the process of single bremsstrahlung and cosmic triggers. Besides that the

process of three-photon annihilation contributes to the hard part of the spectrum, when one photon only is detected.

For the search of bosons with a mass not greater than 200 MeV events were considered which had a photon with an energy close to that of the beam. The insert to the Fig.15 shows the expected spectrum of photons with $E_\gamma = E_0$ at 13% energy resolution (FWHM). 61 events were found in the hard part of the spectrum within the limits determined by the resolution: $0.9 < E_\gamma/E_0 < 1.15$. The detection efficiency for such photons assuming the angular distribution $dN = (1+\cos^2\theta)\,d\Omega$ is slightly energy dependent and varies from 16% to 21% throughout the whole energy range. The energy dependence of the total cross section is presented in Fig.16a and is well described by a constant $\sigma_{tot} = (0.24 \pm 0.03)$ nb. Since quantitative subtraction of the background has not been performed this result corresponds to the following upper limit on the cross section at 90% C.L.:

$$\sigma(e^+e^- \to X\gamma) < 0.3 \text{ nb at } 0.9 < E_\gamma/E_0 < 1.15$$

Similar analysis for a softer part of the photon spectrum (Fig.15) corresponding to the X-boson mass up to 800 MeV gives the following upper limits (Figs.16b,c):

$$\sigma(e^+e^- \to X\gamma) < 0.4 \text{ nb at } 0.75 < E_\gamma/E_0 < 0.9$$
$$\sigma(e^+e^- \to X) < 0.8 \text{ nb at } 0.6 < E_\gamma/E_0 < 0.75$$

In conclusion the authors express their sincere gratitude to the staff of the computing center and VEPP-2M for the joint work during many years.

REFERENCES

1. *G.M.Tumaikin.* Proceedings of the 10 International Conference on High Energy Particle Accelerators, V.1, p.443, Serpukhov, 1977.
2. *V.M.Aulchenko et al.* Preprint INP 82-142, Novosibirsk, 1982, submitted to Nuclear Instruments and Methods.
3. *A.D.Bukin et al.* Preprint INP 83-80, Novosibirsk, 1983.
4. *V.P.Druzhinin et al.* Preprint INP 84-57, Novosibirsk, 1984.
5. *V.P.Druzhinin et al.* Preprint INP 84-62, Novosibirsk, 1984.
6. *J.Berge et al.* Rev. Sci. Instr. 32(1961)538.
7. Review of Particle Properties, Particle Data Group, 1982.
8. *I.B.Vasserman et al.* Phys. Lett. 99b(1981)62.
9. *V.B.Golubev et al.* Report at the 3 International Conference on Colliding Beam Instrumentation, Novosibirsk, 1984.
10. *V.S.Fadin and E.A.Kuraev.* Preprint INP 84-44, Novosibirsk, 1984.
11. *S.I.Eidelman and E.A.Kuraev.* Phys. Lett. 80B (1978)94.
12. *L.M.Kurdadze et al.* Yadernaya Fizika 40(1984)451.
13. *C.H.Lai and C.Quigg.* Preprint FN-296, Fermilab USA, 1976.
14. *M.V.Terentiev.* Uspekhi Fizicheskikh Nauk 112(1974)37.
15. *A.A.Belkov et al.* Submitted to Yadernaya Fizika.
16. *A.I.Vainshtein and I.B.Khriplovich.* Yadernaya Fizika 13(1971)620; *V.N.Novikov and S.I.Eidelman.* Yadernaya Fizika 21 (1975) 1029.
17. *V.N.Baier and V.A.Khoze.* ZhETP 48 (1965) 1708.
18. *J.Yellin.* Phys.Rev. 147(1966) 1080.
19. *H.Levy and P.Singer.* Phys.Rev. 3D (1971)2134.
20. *L.M.Kurdadze et al.* Preprint INP 79-69, Novosibirsk, 1979.
21. *G.Cosme et al.* Phys. Lett. 63B (1976)349.
22. *Y.Layssac and F.M.Renard.* Nuovo Cimento Lett. 1(1971)197.
23. *W.A.Bardeen et al.* Phys. Lett. 76B(1978)580.
24. *P.Fayet and M.Mezard.* Phys. Lett. 104B(1981)226.
25. *L.B.Okun.* Preprint ITEF-149, Moscow, 1983.

Table 1

Cross sections of pion events before and after selection
$E = 510$ MeV

Process	$e^+e^- \to e^+e^-$	$e^+e^- \to \mu^+\mu^-$	$\Phi \to \pi^+\pi^-\pi^0$	$\Phi \to K_S K_L$	$e^+e^- \to \pi^+\pi^-$
σ_{viz}, nb before selection	360	4.8	0.34	5.5	22
σ_{viz}, nb after selection	<0.11	0.26	0.11	0.15	7.3

Table 2

$2E_0$, GeV	L, nb^{-1}	$N_{4\gamma}$	$N_{5\gamma}$	$\varepsilon^{4\gamma+5\gamma}$, %	$\sigma_{tot}^{\omega\pi^0}$ nb	$\sigma_{tot}^{\pi^+\pi^-\pi^0\pi^0}$, nb [20]
1.00÷1.05	2750			2.4	14±3	8±3
1.05÷1.08	131	0	3	2.85	9±5	10±3
1.08÷1.12	133	5	3	3.1	22±8	12±2
1.12÷1.16	153	6	1	3.35	16±6	13±2
1.16÷1.20	156	2	3	3.55	10±5	20±3
1.20÷1.24	160	5	6	3.8	21±6	19±2
1.24÷1.28	156	7	7	3.8	27±7	23±2
1.28÷1.32	161	5	5	3.55	20±6	22±2
1.32÷1.36	159	4	3	3.2	16±6	30±3
1.36÷1.4	151	4	4	2.7	22±8	27±2

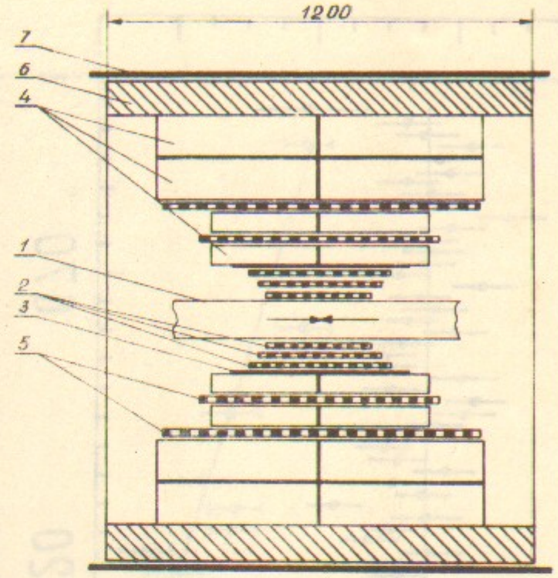

Fig.1. Lay-out of the Neutral Detector: 1—the collider vacuum chamber, 2—coordinate proportional chambers, 3—scintillation counters, 4—NaI(Tl) crystals, 5—shower chambers, 6—iron absorber, 7—anticoincidence counters.

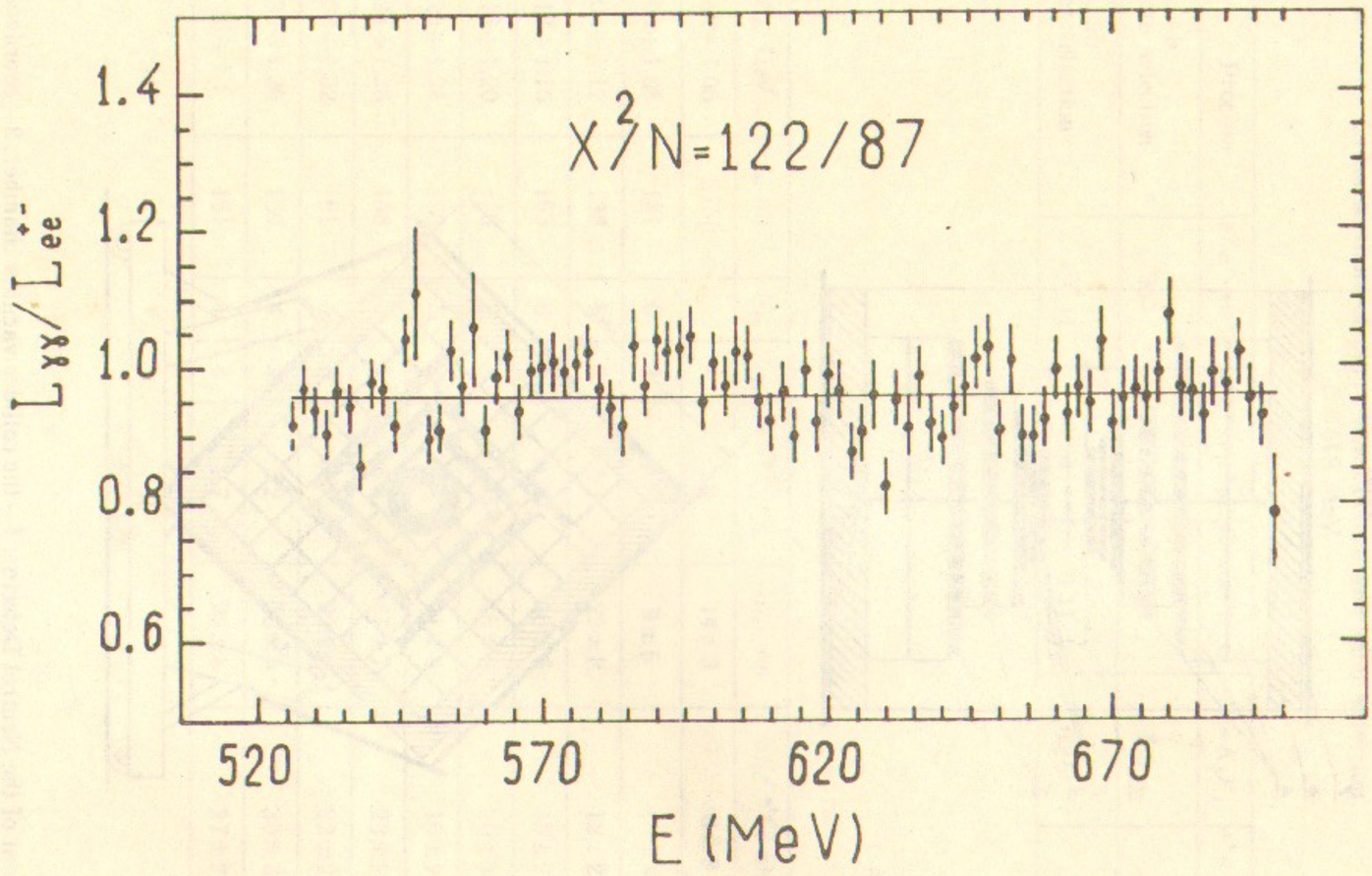

Fig.2. Energy dependence of the ratio of luminosities determined from the two-photon annihilation and large angle Bhabha scattering.

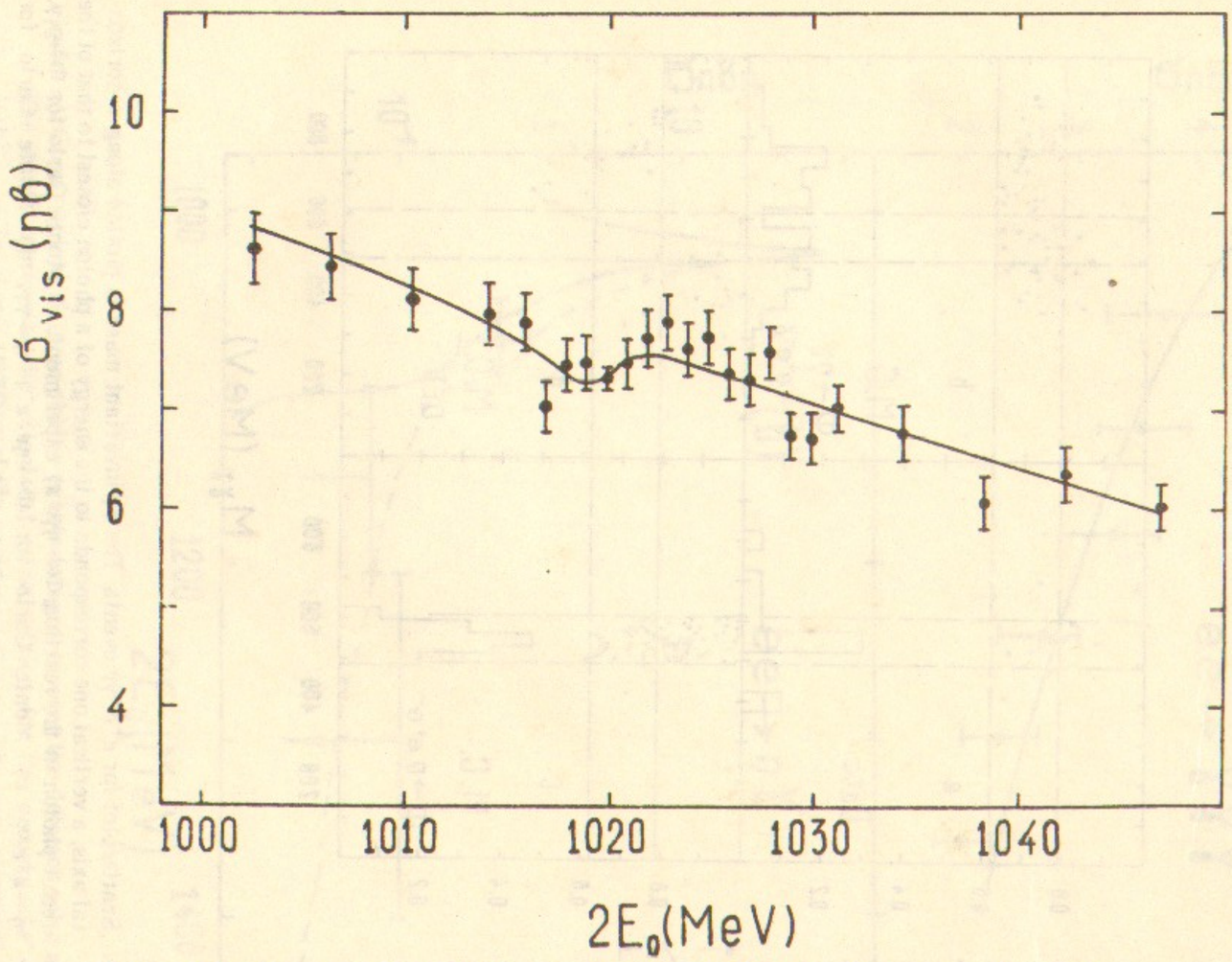

Fig.3. Detection cross section for the process $e^+e^-\to\pi^+\pi^-$. A solid curve is the result of the fit.

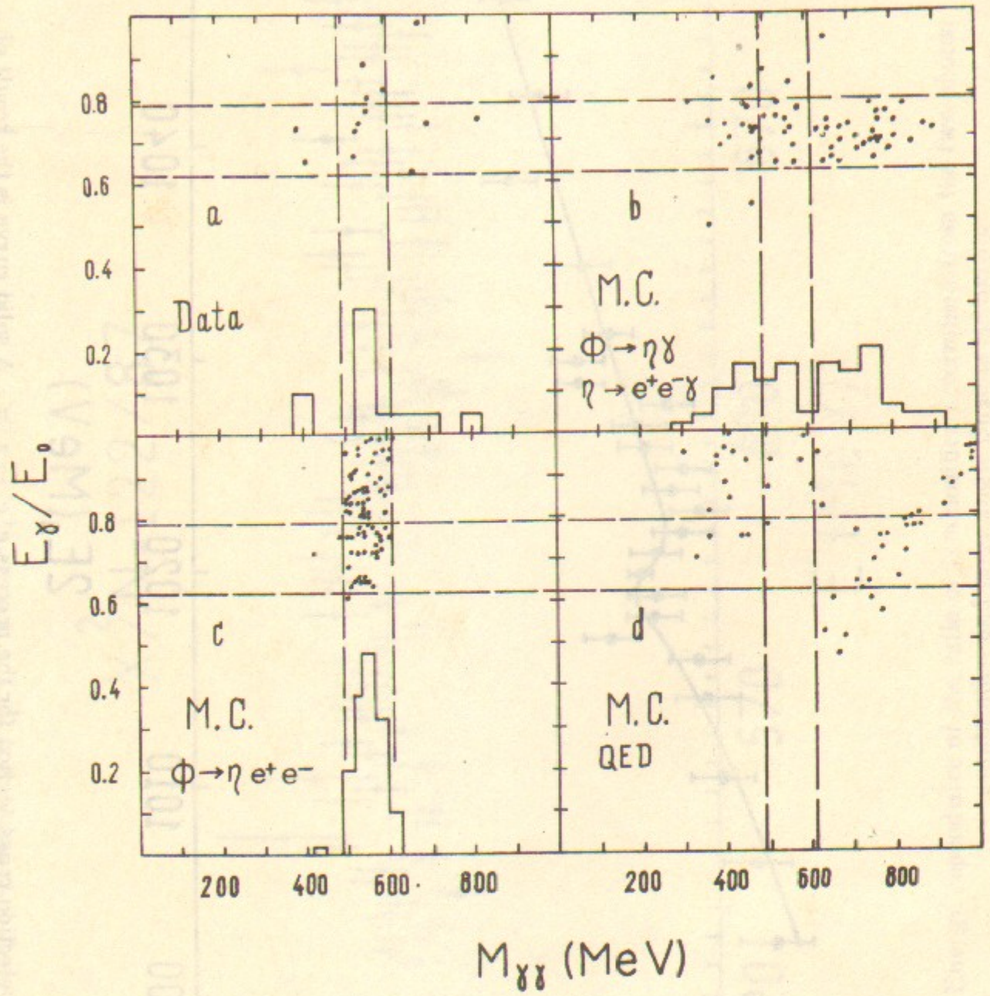

Fig.4. Scatterplot for $e^+e^-\gamma\gamma$ events. The $\gamma\gamma$ invariant mass is plotted along a horizontal axis, a vertical one corresponds to the energy of a photon closest to that of the recoil photon in the reaction $\Phi\to\eta\gamma$: a) experiment, b) Monte Carlo for $\Phi\to\eta\gamma$, $\eta\to e^+e^-\gamma$; c) Monte Carlo for $\Phi\to\eta e^+e^-$, $\eta\to\gamma\gamma$, d) Monte Carlo for $e^+e^-\to e^+e^-\gamma\gamma$ (QED).

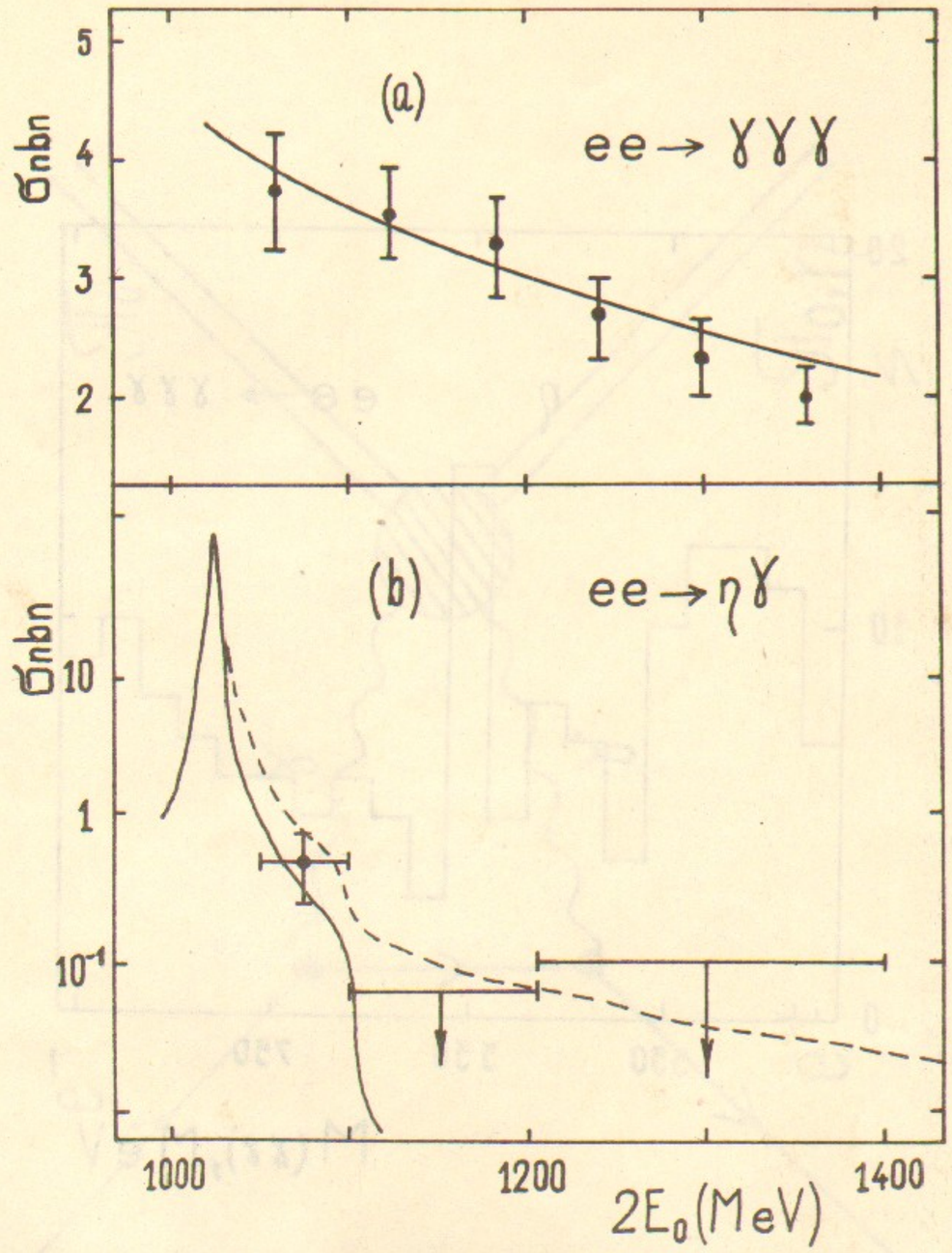

Fig.5. a) Cross section of three-photon events integrated over the detector solid angle. The curve represents the calculated cross section for the process $e^+e^-\to\gamma\gamma\gamma$ (QED); b) Total cross section of the process $e^+e^-\to\eta\gamma$. The lines represent ϱ and Φ-meson contributions. The solid line corresponds to the destructive interference, the dashed line—to the constructive one.

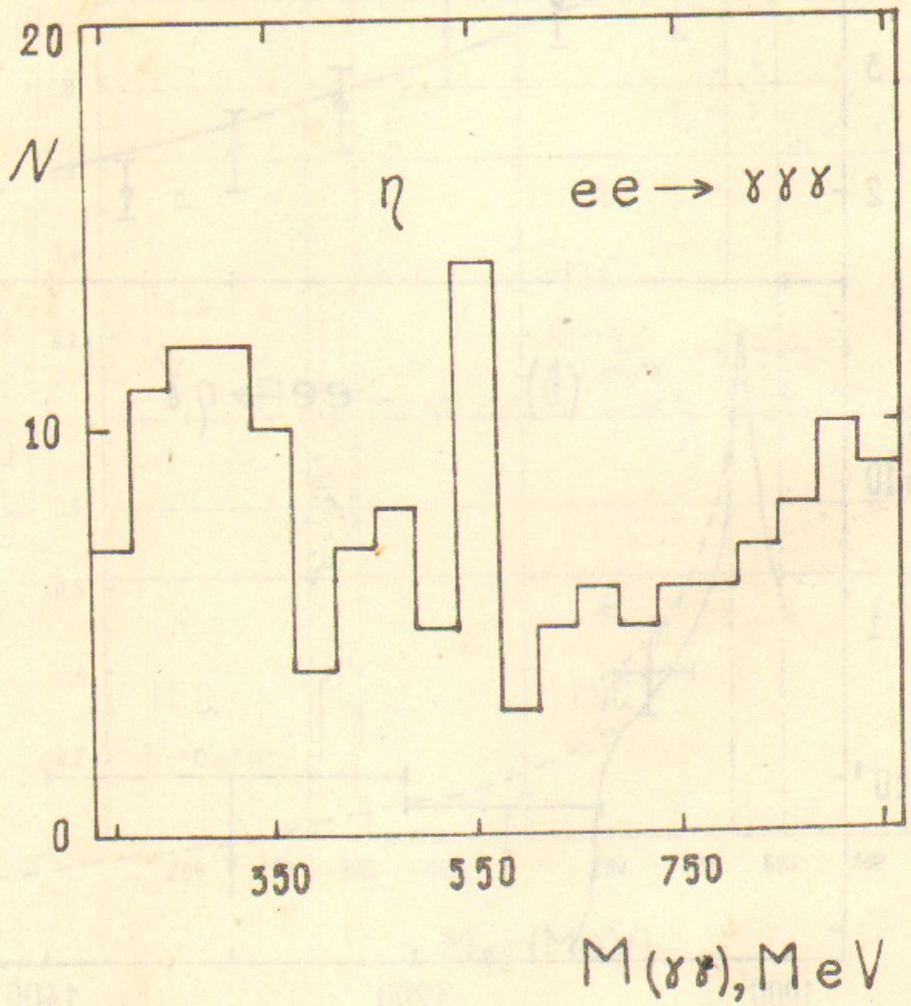

Fig.6. Diphoton masses for three-photon events in the energy range between 1050 and 1100 MeV.

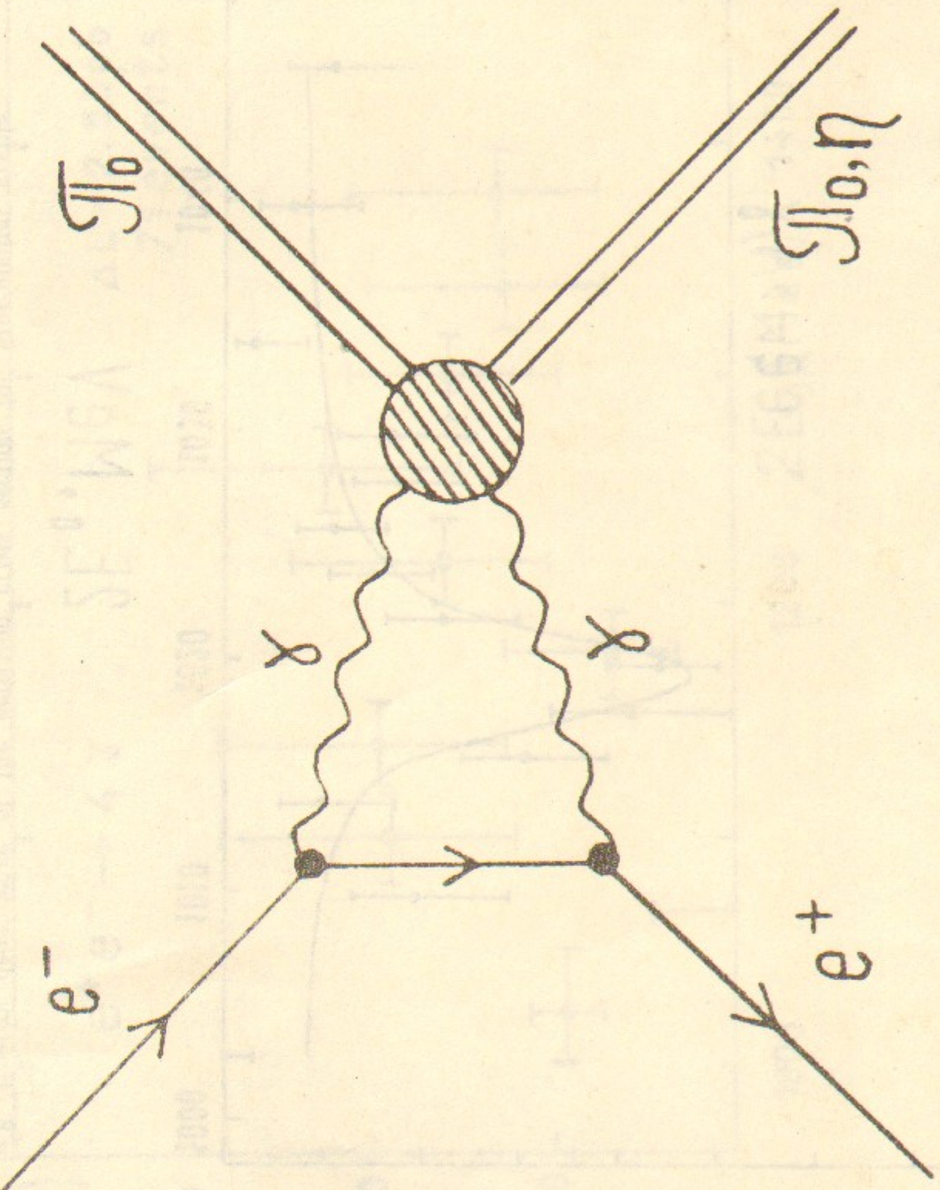

Fig.7. Diagram for the reaction $e^+e^- \to \pi^0\pi^0$ due to the polarizability of the π^0-meson.

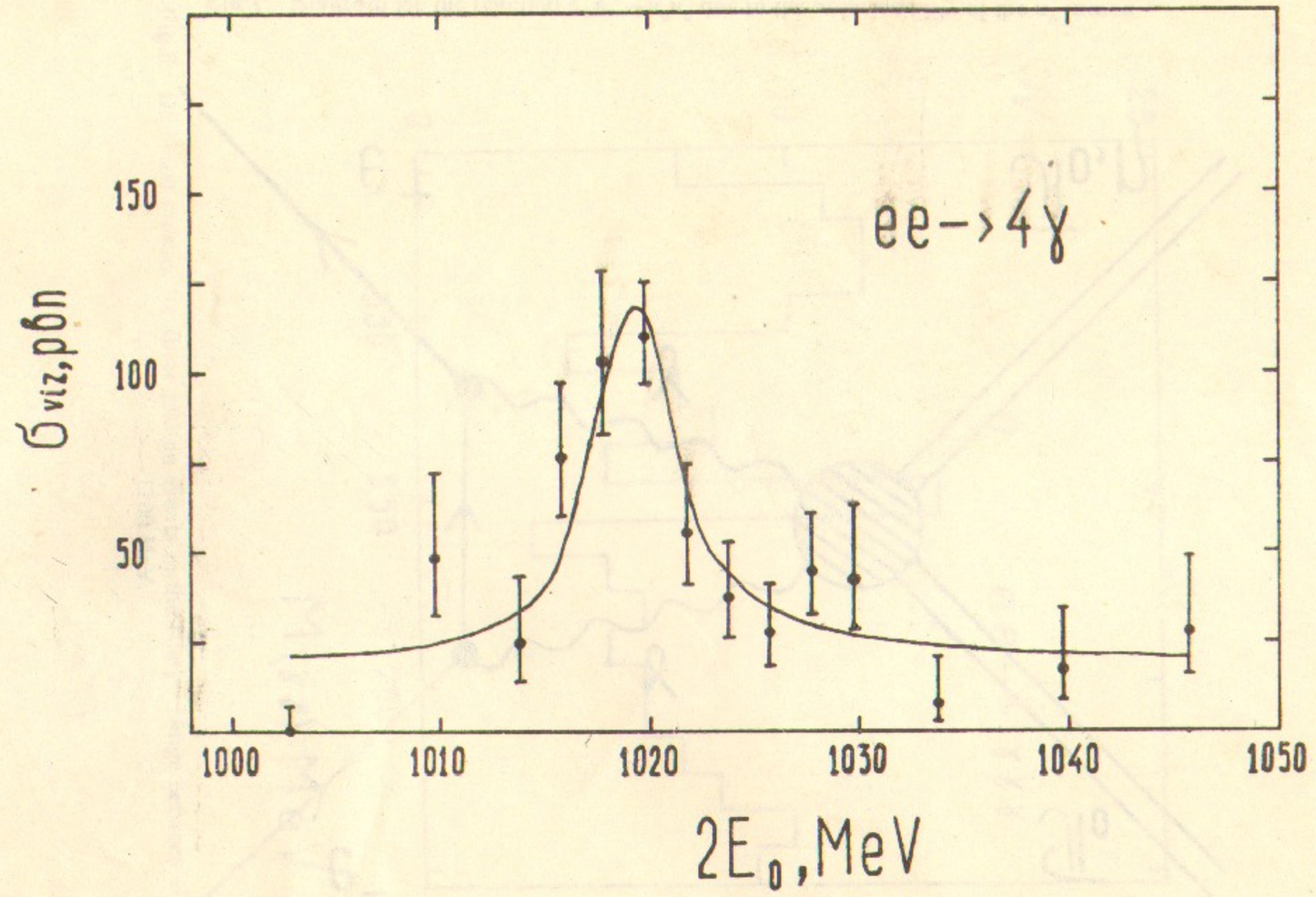

Fig.8. Energy dependence of the detection cross section for four-photon events ($2E_0 = 1000—1050$ MeV).

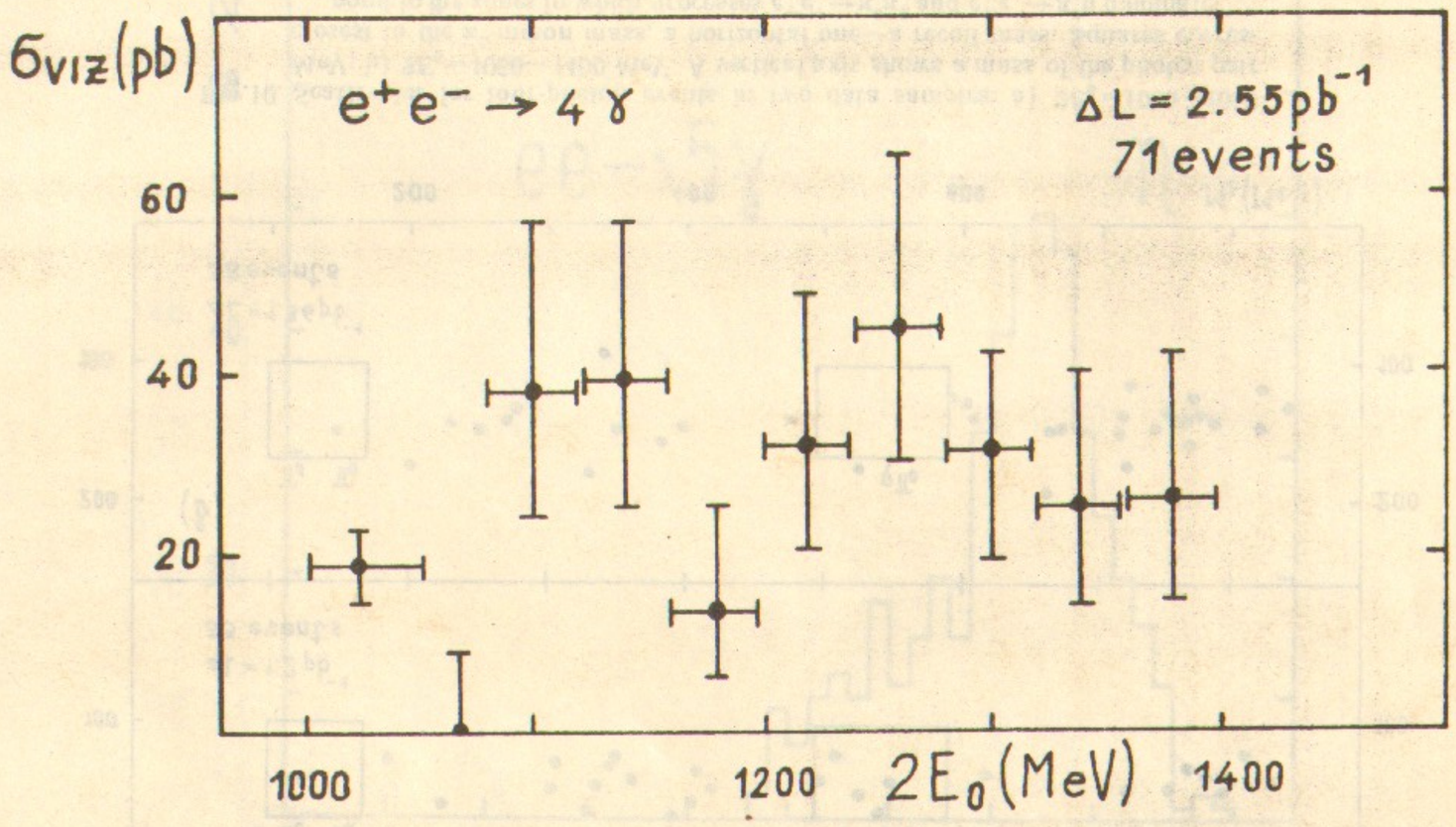

Fig.9. Energy dependence of the detection cross section for four-photon events ($2E_0 = 1050—1400$ MeV).

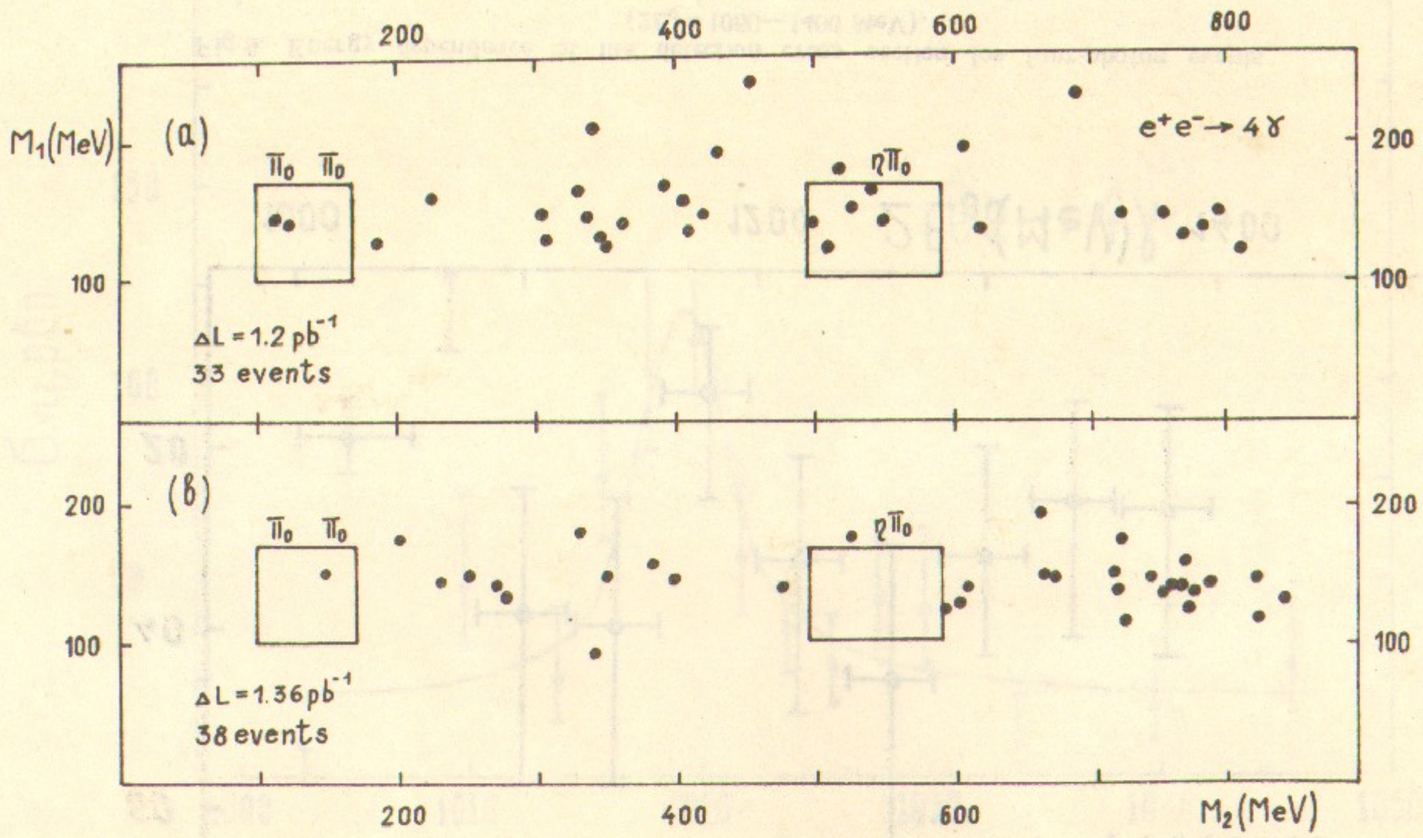

Fig.10. Scatterplot for four-photon events in two data samples: a) $2E_0 = 1000—1050$ MeV, b) $2E_0 = 1050—1400$ MeV. A vertical axis shows a mass of the photon pair closest to the π^0-meson mass, a horizontal one—a recoil mass. Squares correspond to the zones in which processes $e^+e^- \to \pi^0\pi^0$ and $e^+e^- \to \pi^0\eta$ dominate.

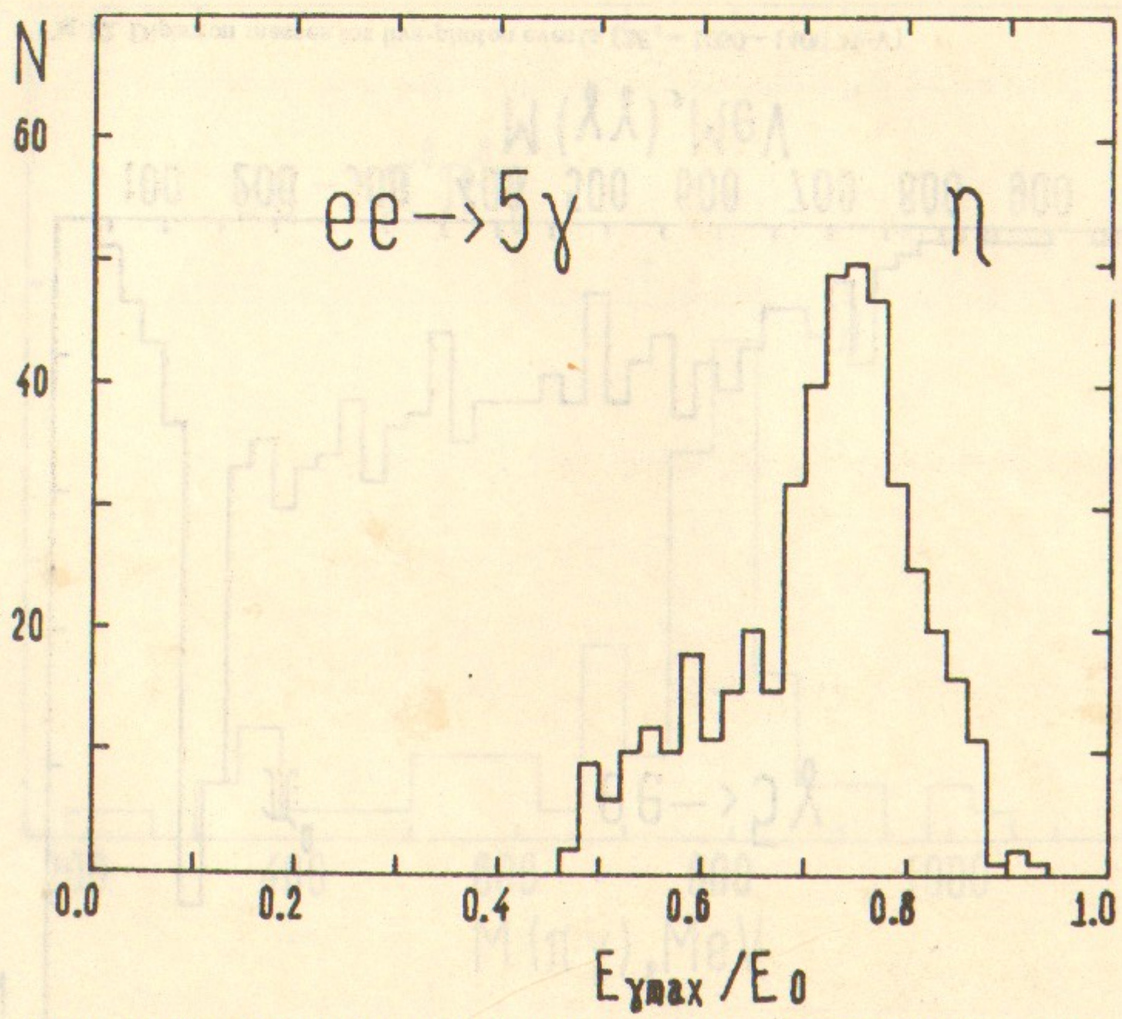

Fig.11. Energy spectrum of the photons with a maximum energy in five-photon events ($2E_0 = 1000—1050$ MeV).

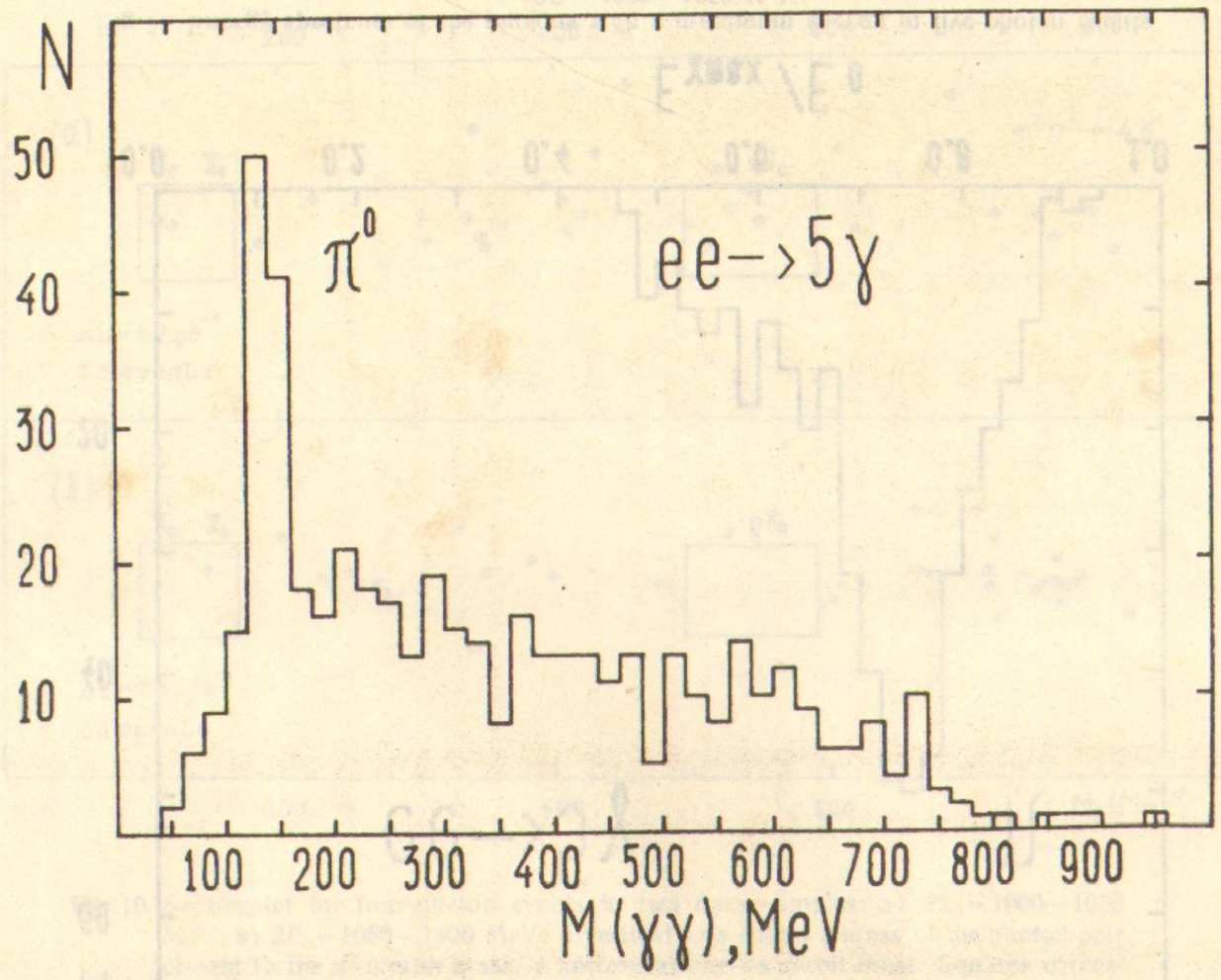

Fig.12. Diphoton masses for five-photon events ($2E_0$= 1050—1400 MeV).

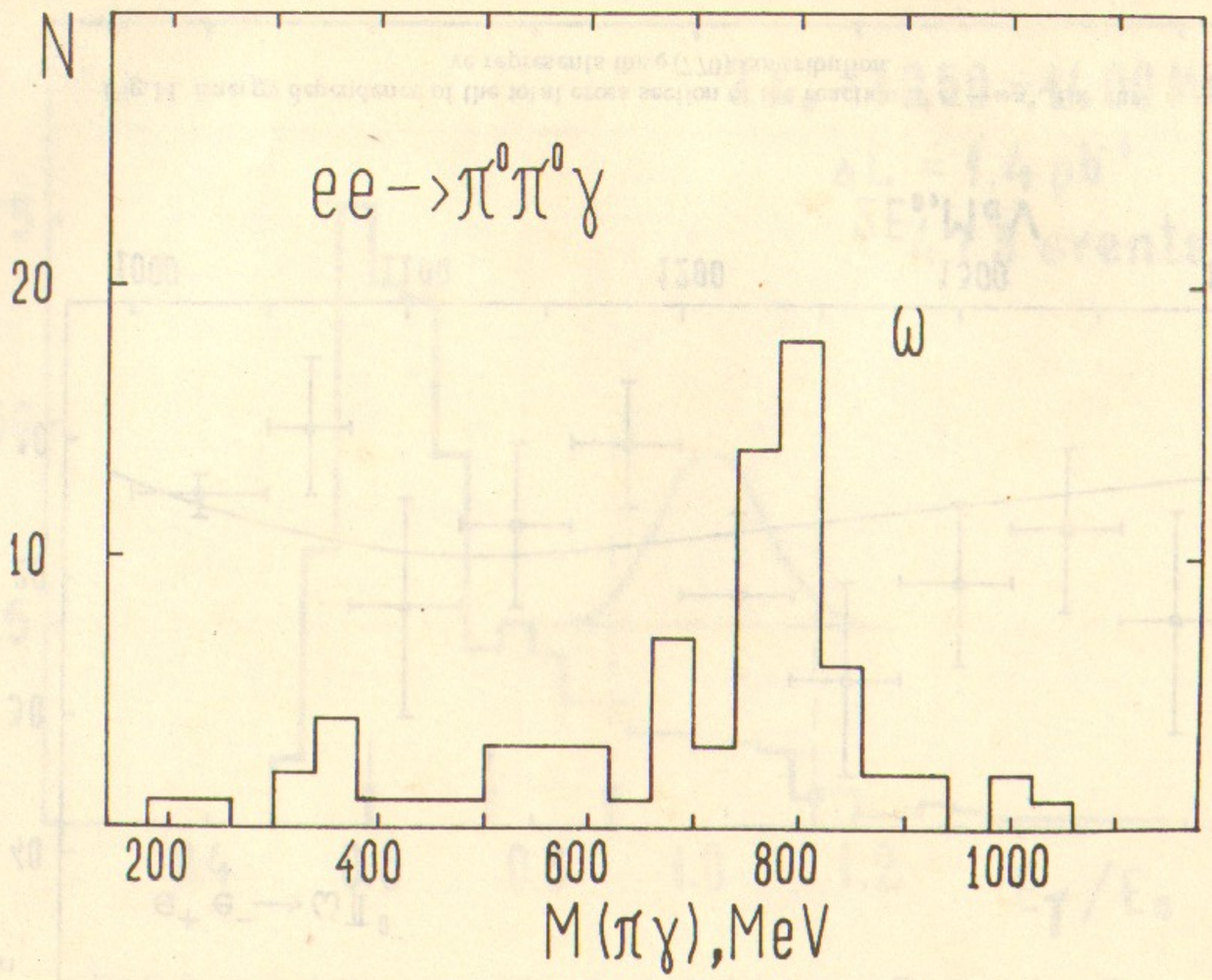

Fig.13. $\pi^0\gamma$ masses in five-photon events with two π^0-mesons.

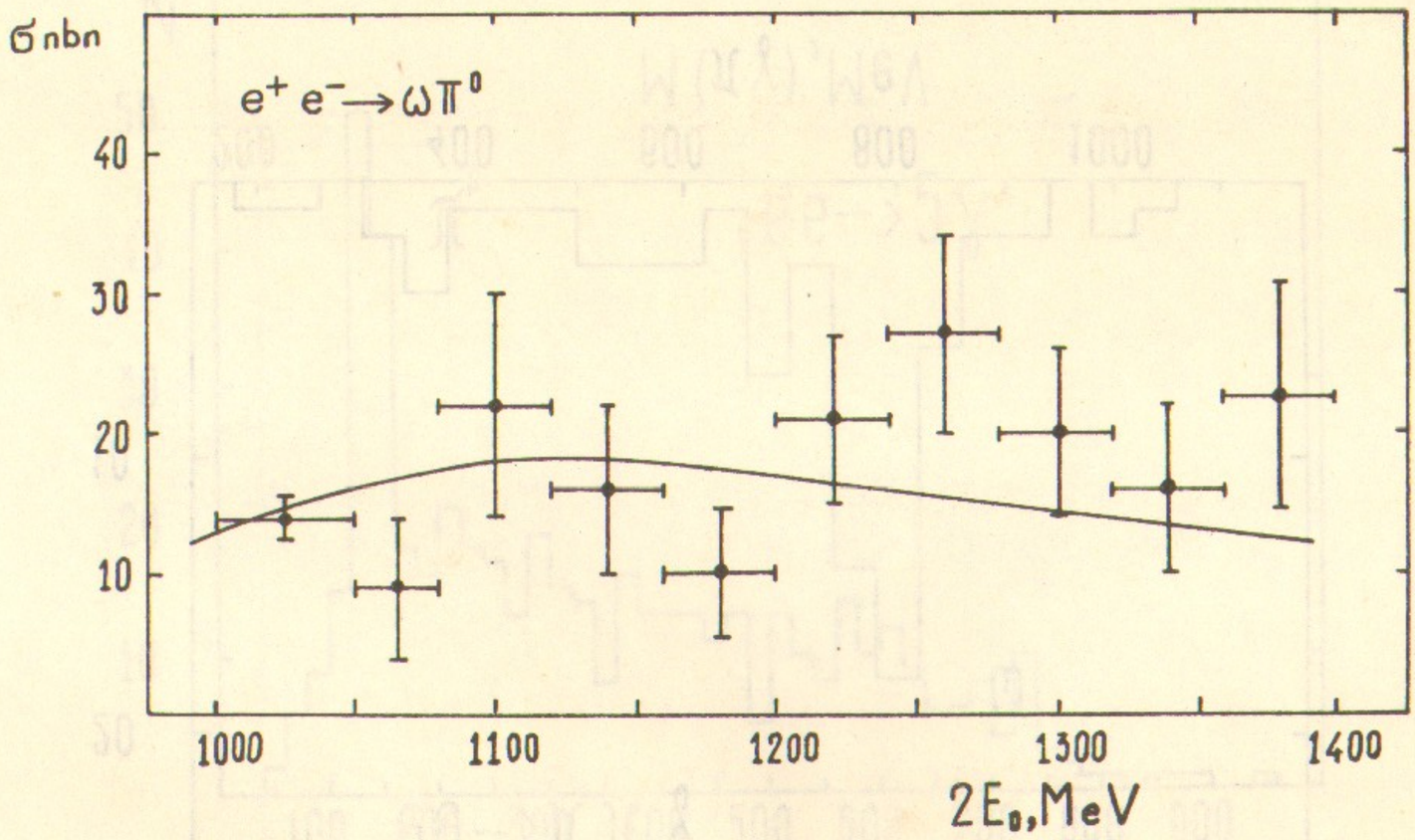

Fig.14. Energy dependence of the total cross section of the reaction $e^+e^- \to \omega\pi^0$. The curve represents the $\varrho(770)$ contribution.

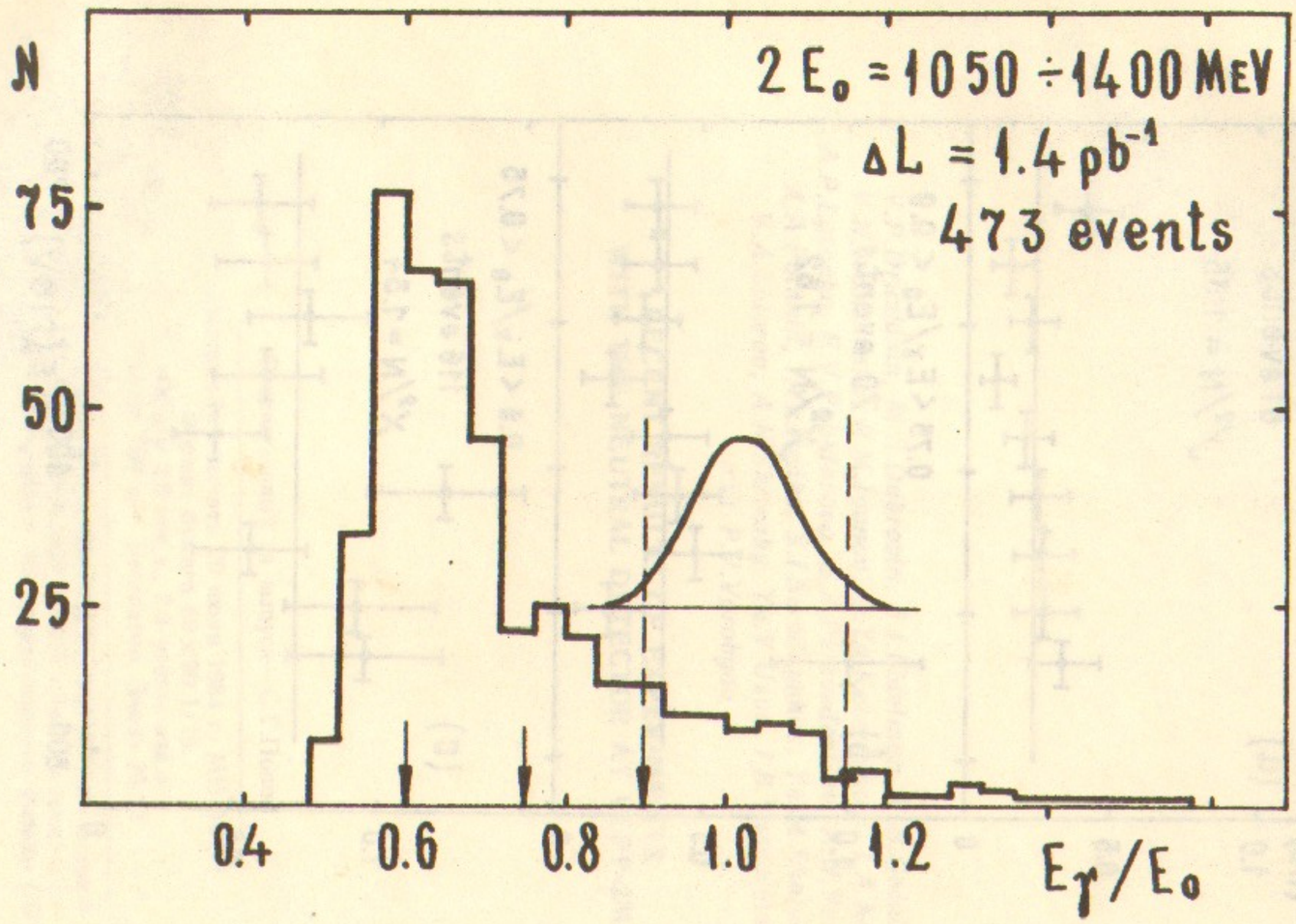

Fig.15. Inclusive photon energy spectrum for single photon events. The insert shows the expected photon spectrum for production of particles with a mass not greater than 200 MeV. Arrows indicate the boundaries of the photon energy intervals.

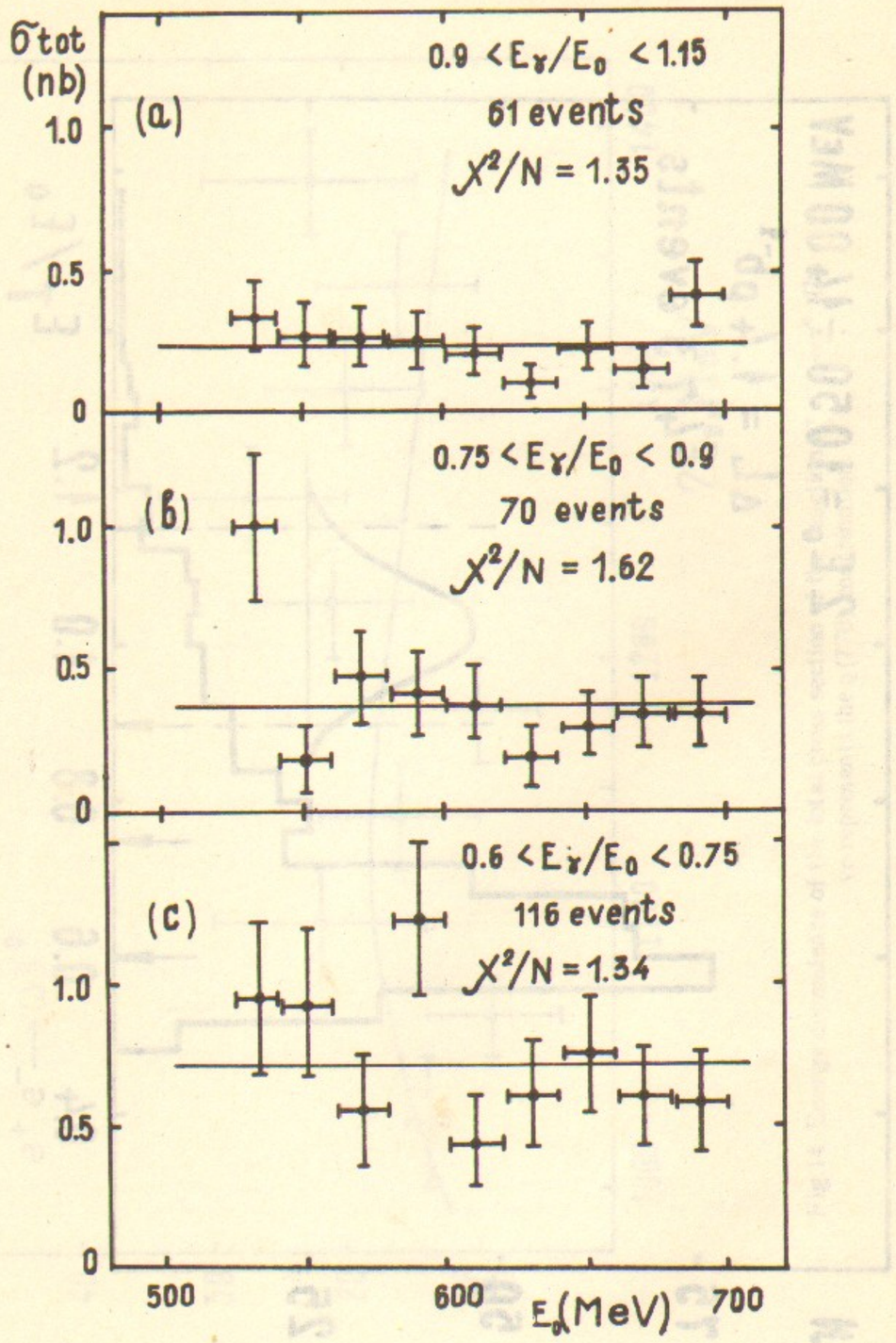

Fig.16. Energy dependence of the total cross section for single photon events at different photon energies.

V.P.Druzhinin, M.S.Dubrovin, S.I.Eidelman, V.B.Golubev, V.N.Ivanchenko, R.M.Ivanov, G.Ya.Kezerashvili, I.A.Koop, A.P.Lysenko, E.V.Pakhtusova, E.A.Perevedentsev, A.N.Peryshkin A.A.Polunin, I.Yu.Redko, S.I.Serednyakov, Yu.M.Shatunov, V.A.Sidorov, A.N.Skrinsky, Yu.V.Usov, I.B.Vasserman, and P.V.Vorobyov

RECENT RESULTS OF EXPERIMENTS WITH THE NEUTRAL DETECTOR AT VEPP-2M

Ответственный за выпуск—С.Г.Попов

Подписано в печать 20 июня 1984 г. МН 04396
Формат бумаги 60×90 1/16.
Объем 2,8 печ.л., 2,3 учетно-изд.л.
Тираж 290 экз. Бесплатно. Заказ № 93

Набрано в автоматизированной системе на базе фотонаборного автомата ФА-1000 и ЭВМ «Электроника» и отпечатано на ротапринте Института ядерной физики СО АН СССР,
Новосибирск, 630090, пр. академика Лаврентьева, 11